Transactions of JWRI, Vol.36 (2007), No. 2

Numerical Simulation of Metal Vapor Behavior in Argon TIG Welding†

YAMAMOTO Kentaro*, TANAKA Manabu**, TASHIRO Shinichi***,
NAKATA Kazuhiro**** and MURPHY A. B. *****

Abstract

A gas tungsten arc in argon is modeled taking into account the contamination of the plasma by the metal vapor from the weld pool surface. The whole region of gas tungsten arc welding, namely the tungsten cathode, arc plasma and weld pool, is treated using a unified numerical model. A viscosity approximation is used to express the diffusion coefficient in terms of the viscosities of the argon gas and the iron vapor. The time-dependent two-dimensional distributions of temperature, velocity and iron vapor concentration are predicted, together with the weld penetration as function of time for a 150 A arc at atmospheric pressure.

KEY WORDS: (Simulation) (Gas Tungsten arc) (Argon) (Metal Vapor) (Welding)

1. Introduction

During the arc welding process, four states of matter, solid, liquid, gas and plasma, simultaneously exist and mutually interact within a volume of only 1 cm^3. The temperature range is wide, ranging from about 20 000 K in the arc plasma, about 3000 K in the tungsten cathode, about 2000 K in the molten steel, down to room temperature in the surrounding regions [1]. Due to the remarkable progress in computer simulation and observation techniques recently, it has become possible to understand the phenomena in arc welding processes quantitatively [2, 3]. However, it has not been possible to accurately predict the welding parameters, such as the arc voltage and the weld geometry. For a full understanding and accurate prediction of these parameters, it is necessary to understand the behavior of metal vapor in the arc plasma.

Metal atoms generally have more low-energy excited states, and are more easily ionized, than atoms of shielding gases such as argon and helium. These characteristics contribute to an increase of the radiative emission coefficient and the electric conductivity of the plasma. It is estimated that the former affects the thermal pinch effect and the energy efficiency of the arc plasma and that the latter affects the current density distribution. Tashiro et al. [4] conducted a virtual experiment by numerically simulating a pure helium arc and an arc in helium uniformly mixed with 30 mol% iron atoms, and showed that an obvious arc constriction occurred for the latter case. Furthermore, they reported that the energy efficiency greatly decreased from about 80% to about 35%. These results suggested that existence of metal vapor changed the heat source property in the arc welding process, and consequently changed the size and the shape of the molten pool.

As noted above, there have been significant advances in the simulation of arc welding. For example, a numerical simulation of gas metal arc welding, including the formation of droplets from a steel wire electrode, has been reported [5]. However, the effect of metal vapor was not considered. On the other hand, calculations of the behavior of metal vapor in an atmospheric pressure plasma have also been reported [6]. However, the conditions were far from those occurring in welding because a solid electrode with constant temperature was assumed. It is important for accurate understanding of the arc welding process to consider the mixing of the metal vapor in a model that takes into account the tungsten cathode, the arc plasma and the weld pool.

In the present paper, we use a numerical model of stationary gas tungsten arc (GTA) welding taking into account the iron vapor produced from the weld pool surface, and we simulate the distribution of the metal vapor, the plasma temperature and the formation of the weld pool in GTA welding.

† Received on December 14, 2007
* Graduate Student
** Associate professor
*** Designated Researcher
**** Professor
***** Materials Science and Engineering, CSIRO
Transactions of JWRI is published by Joining and Welding Research Institute, Osaka University, Ibaraki, Osaka 567-0047, Japan

2. Simulation Model

The tungsten cathode, arc plasma and anode are described relative to cylindrical coordinates, assuming rotational symmetry around the arc axis. The calculation domain is shown in **Fig. 1**. The diameter of the tungsten cathode is 3.2 mm with a 60 degrees conical tip. The anode is of stainless steel. Argon shielding gas is introduced from the outside of the cathode on the upper boundary at the flow rate of 10 L/min.

The convection in the weld pool is influenced by the shear stress due to the convective flow of the cathode jet, the Marangoni force due to the gradient in the surface tension of the weld pool, buoyancy due to gravity and the electromagnetic pinch force due to the arc current. Only the driving forces of the weld pool convection at the boundary between the weld pool and the arc plasma are explained here. First, the shear stress is already included in radial momentum conservation through the viscosity at the anode surface. Second, the Marangoni force is given by [7]

$$M_A = \frac{\partial}{\partial z}\left(\frac{\partial \gamma}{\partial T}\frac{\partial T}{\partial r}\right) \tag{1}$$

where T is temperature, γ is the surface tension of the weld pool. In this paper, stainless steel is assumed to have low sulfur content (about 10 ppm) and the variation of the surface tension at the weld pool surface is assumed to decrease linearly with increasing temperature ($\partial\gamma/\partial T = -0.46mN/mK$) [7].

A species conservation equation expressed by equation (2) is applied to take into account the metal vapor behavior [6]. In practice, metal vapor species in an arc plasma with a stainless steel anode include Fe, Cr, Ni, Mn and so on [8]. However, to simplify the model and facilitate calculation, only iron vapor is considered in this model.

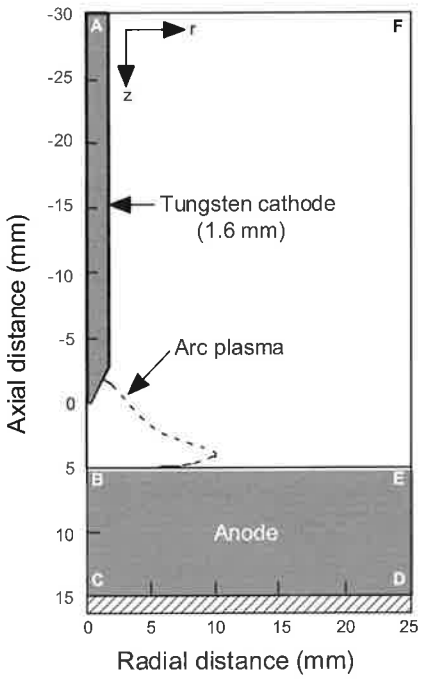

Fig. 1 Schematic illustration of simulation domain.

$$\frac{\partial}{\partial t}(\rho C_1) + \frac{1}{r}\frac{\partial}{\partial r}(r\rho v_r C_1) + \frac{\partial}{\partial z}(\rho v_z C_1) = \frac{1}{r}\frac{\partial}{\partial r}\left(r\rho D\frac{\partial C_1}{\partial r}\right) + \frac{\partial}{\partial z}\left(\rho D\frac{\partial C_1}{\partial z}\right) \tag{2}$$

where t is time, v_r and v_z are the radial and axial velocities, ρ is the density, C_1 is mass fraction concentration of iron vapor and D is the binary diffusion coefficient, which is expressed by the viscosity approximation equation:

$$D = \frac{2\sqrt{2}\left(1/M_1 + 1/M_2\right)^{0.5}}{\left\{\left(\rho_1^2/\beta_1^2\eta_1^2 M_1\right)^{0.25} + \left(\rho_2^2/\beta_2^2\eta_2^2 M_2\right)^{0.25}\right\}^2} \tag{3}$$

where M_1 and M_2 are the molecular weights of iron and the argon gas respectively. Similarly, ρ_1, ρ_2, η_1, η_2 are respectively the density and viscosity of iron and the argon gas. β_1, β_2 are the dimensionless constants defined as $\beta_i = (D_{ii}\rho_i)/\eta_i$, and theoretically range from 1.2 to 1.543 for various species of gas, such as Ar, He, H_2, N_2, O_2, CO_2 and so on. It is assumed that $\beta_1 = \beta_2 = 1.385$, which is based on the mean value of experimental data [9]. The viscosity approximation is not strictly justified since it does not take into account ionized species but is at best reasonably accurate [10]; however it is considered to be a useful first approximation for the arc welding model.

C_1 is set to be zero in the cathode area and in the solid area of the anode. However, at the anode surface where the temperature is above the melting point, C_1 is set to [6]:

$$C_1 = \frac{p_{v,1}M_1}{p_{v,1}M_1 + (p_{atm} - p_{v,1})M_2} \tag{4}$$

where p_{atm} is atmospheric pressure and $p_{v,1}$ is the iron vapor partial pressure, which is a function of the weld pool temperature. According to equation (4), C_1 has values between zero and 1.0. For other boundary conditions, C_1=0 at AF and FE shown in Fig. 1, and $(\partial C_1/\partial r) = 0$ at the arc axis (AB).

In the present model, plasma properties are dependent on not only the temperature but also the mole fraction of iron vapor. Plasma properties at intermediate concentrations of iron vapor are calculated using a linear approximation based on the properties at 0 mol%, 1 mol%, 10 mol%, 20 mol% and 30 mol% [12]. The properties were calculated assuming the arc plasma to be in the local thermodynamic equilibrium (LTE), and using the Chapman-Enskog approximation [12]. For example, the electrical conductivities, which are significantly affected, are shown in **Fig. 2**. The electrical conductivities are greatly increased by the addition of iron vapor at temperatures below 8 000 K, and the values for mixing ratios 1%, 10%, 20% and 30% are almost the same.

The other approximations, governing equations and

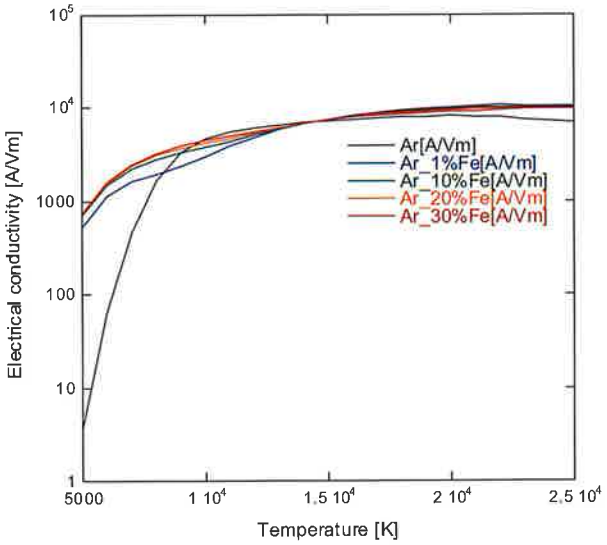

Fig. 2 Dependence of electrical conductivities of argon gas on temperature for each mixing ratio.

boundary conditions are given in detail in our previous papers [4, 13]. The governing and auxiliary equations are solved iteratively by the SIMPLEC numerical procedure.

3. Calculated Results

The present model is applied to the case of stationary argon GTA welding of stainless steel. **Figure 3** shows the two-dimensional distribution of temperature, fluid flow velocity and mole fraction of iron vapor at a time 20 s after arc ignition, namely, when the weld pool has grown to a reasonable extent. The distribution of iron vapor depends on the diffusion term and the convection term, as described in Eq. (2). Due to the cathode jet,

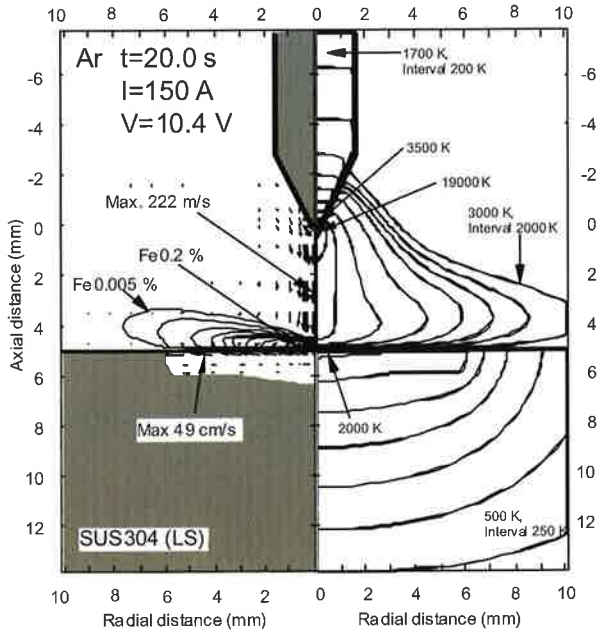

Fig. 3 Calculated results for argon GTA welding for 150 A at 20 s after arc ignition.

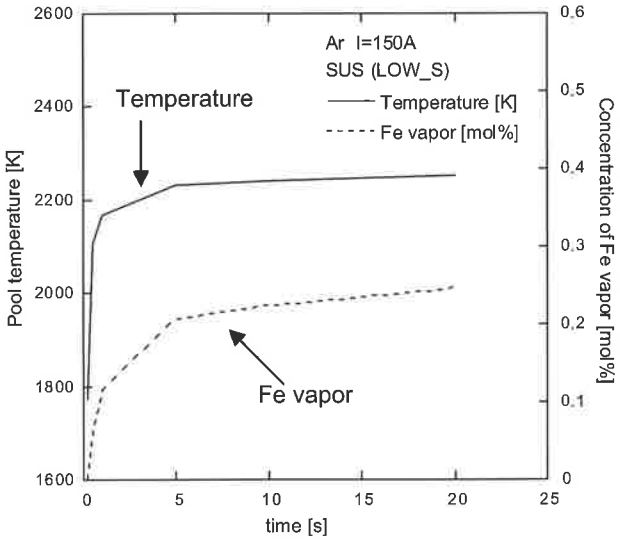

Fig. 4 Relation between maximum weld pool temperature and maximum concentration of iron vapor in argon GTA welding.

which leads to flow velocities of over 200 m/s in the welding arc, the convection term has a strong effect. Therefore, it is found that distribution of iron vapor expands in the radial direction and is concentrated around the weld pool surface. The concentration of iron vapor in the arc plasma is up to 0.2 mol%.

Figure 4 shows the maximum concentration of iron vapor in the arc plasma, obtained from time-dependent calculation. The maximum temperature of the weld pool is also shown. This figure shows iron vapor concentration increases with increased weld pool temperature. The weld pool temperature is about 2200 K, which is a very low temperature. Thus, the maximum concentration of iron

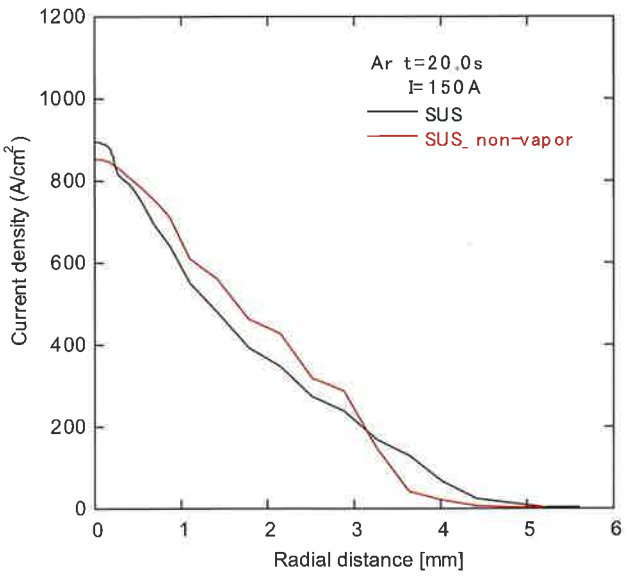

Fig. 5 Comparison of calculated current densities at the anode surface.

vapor is significantly small, about 0.25 mol%.

Figure 5 shows current density distributions at the anode surface for the stainless steel anode and the distribution calculated neglecting the effect of iron vapor on the arc plasma is also given. For the stainless steel anode, the peak current density is 895 A/cm^2, which is not obviously different from that neglecting the iron vapor, because the iron vapor concentration in arc plasma is significantly small in argon GTA welding. However, the region through which current flows is slightly expanded by the increase of the electric conductivity at lower temperatures; as shown in Fig. 2, the increase is greater at the lower temperatures that occur away from the arc axis.

4. Conclusion

We have used a numerical model of a stationary GTA welding taking into account the iron vapor from the weld pool surface, and have simulated the effect of the iron vapor on the properties of the arc. The main conclusions are summarized as follows:

(1) Due to the cathode jet velocity of over 200 m/s in the welding arc, the convection term strongly affects the distribution of the iron vapor. It was found that iron vapor expanded mainly in the radial direction and remained concentrated around the weld pool surface.

(2) The maximum concentration of iron vapor is significantly small, about 0.25 mol% because the weld pool temperature is very low.

(3) Current density distribution at the anode surface in argon GTA welding is not obviously different from that neglecting the iron vapor, because the iron vapor concentration in arc plasma is significantly small. However, the region through which current flows is slightly expanded by the increase of the electric conductivity at lower temperatures.

References

1) M. Tanaka, et al: *J. Plasma & Fusion Res.*, 82-8 (2006), 492-496 (in Japanese).
2) H.G. Fan, et al: *Quarterly J. Japan Welding Soc.*, 76-2 (2007), 82-89.
3) H. Nishiyama, et al: *ISIJ Int.*, 46-5 (2006), 705-711.
4) S. Tashiro, et al: *Quarterly J. Japan Welding Soc.*, 24-2 (2006), 143-148 (in Japanese).
5) H.G. Fan, et al: *J. Phys. D: Appl. Phys.*, 37 (2004), 2531-2544.
6) J. Menart, et al: *Plasma Chem. & Plasma Process.*, 19-2 (1999), 153-170.
7) M. Tanaka, et al: *J. Phys. D: Appl. Phys.*, 40 (2007), R1-R23.
8) H. Terasaki, et al: *Quarterly J. Japan Welding Soc.*, 20-2 (2002), 201-206.
9) C.R. Wilke: *J. Chem. Phys.*, 18-4 (1950), 517-519.
10) A.B. Murphy: *J. Phys. D: Appl. Phys.*, 29 (1996), 1922-1932.
11) The Japan Institute of Metals: *Edition No. 3 Data Book of Metals*, MARUZEN CO., LTD, (1993) (in Japanese).
12) A.B.Murphy: *Plasma Chem. & Plasma Process.*, 15-2 (1995), 279-307.
13) S. Tashiro, et al: *Quarterly J. Japan Welding Soc.*, 25-1 (2007), 3-9 (in Japanese).